4 (2025) 117–131

Contents lists available at ScienceDirect

Resilient Cities and Structures

journal homepage: www.elsevier.com/locate/rcns

Full Length Article

Integrated flood risk management for urban resilience: A multi-method framework combining hazard mapping, hydrodynamic modelling, and economic impact assessment

Paboda Jayawardane [a], Lalith Rajapakse [a,*], Chandana Siriwardana [b]

[a] Department of Civil Engineering, University of Moratuwa, Moratuwa, Sri Lanka
[b] School of Built Environment, Massey University, Auckland, New Zealand

ARTICLE INFO

Keywords:
Flood damage
Flood mitigation measures
Inundation area
Inundation depth
Vulnerability curves

ABSTRACT

Flooding has become an emerging global catastrophe, generating considerable damage to both infrastructures and lives. Despite the critical need for quantitative assessments of both flood damage and the effectiveness of flood mitigation measures, most existing studies have focused on isolated aspects of flood risk. Only a very limited number of studies have comprehensively integrated hazard mapping, hydrodynamic simulations, and economic damage estimations to evaluate the real-world impact and effectiveness of flood mitigation measures (FMMs). This study presents a multi-method approach to evaluate the performance of such established structural FMMs. Initially, hazard assessments for two selected case study areas, the Colombo Metropolitan Area in Sri Lanka and Auckland, New Zealand, two flood-prone cities with contrasting geographical contexts. Flood inundation mapping for the Madiwela South Diversion, Colombo, Sri Lanka, was performed using hydrodynamic modeling to demonstrate the reduction in flood inundation area and depth after the implementation of the measure, considering six (6) design return periods (RPs). Subsequently, tangible and intangible property damage estimations for "without FMMs" and "with FMMs" were evaluated to identify the benefit of responding to flood conditions, utilising a vulnerability-based economic analysis. In addition to damage estimations, the study adopts a novel approach by conducting an investment viability analysis to find the Benefit-to-Cost ratios and Net Present Value of nine (9) selected FMMs implemented by Sri Lanka Land Development Co-operation (SLLDC). The FMMs implemented by SLLDC were selected from Colombo, Sri Lanka. The quantified damage estimates revealed a reduction in flood damages ranging from 39 % to 63 %, alongside a decrease in flood inundation depths between 9 % and 12 %, and the results underscore the significant effectiveness of FMMs in managing urban flooding and minimising its impacts. This cross-disciplinary methodology enables a transferable framework for resilience-oriented urban planning in diverse hydrological and geographical contexts.

1. Introduction

Flooding has emerged as the most frequent and significant catastrophic event among devastating natural disasters, causing considerable destruction in urban environments in a global context. The limited infiltration in urban areas [1], exacerbated by the impacts of climate change and rapid urbanisation, has intensified urban floods, presenting significant challenges for built environments [2]. Urban flooding is commonly caused by intense precipitation that exceeds the drainage capacity of a basin. This results in the impoundment of water in drainage networks, leading to a sudden surge of water flow at the basin outlets [3]. Such events can cause significant damage to the surrounding areas and infrastructure [4]. Urban infrastructure developments continuously reduce the percentage of pervious ground surfaces, interrupting natural infiltration and resulting in inadequate drainage capacities with altered natural runoff ways [5]. These altered environmental conditions lead rapidly developing urban areas to a highly vulnerable state due to emerging environmental concerns and natural disasters, including flooding [6]. Historical events like Hurricane Helene-induced floods in September 2024, which caused severe damage to the city of Asheville, North Carolina, provide evidence of the destructive nature of urban floods [7], where economic, transportation, commercial, social, and health sectors constitute major problems, including life losses [8].

The Commonwealth Scientific and Industrial Research Organization

* Corresponding author.
E-mail address: lalith@uom.lk (L. Rajapakse).

https://doi.org/10.1016/j.rcns.2025.09.002
Received 31 December 2024; Received in revised form 21 August 2025; Accepted 15 September 2025
Available online 17 October 2025

(CSIRO) announced that the Asian continent is the most often and severely impacted continent due to extreme flooding. Similarly, countries like Austria, Australia, China, Italy, New Zealand, the UK, and the USA also faced several unexpected extraordinary flood conditions throughout 2020-2023, which highlights the intensification of urban floods in terms of occurrence frequency and intensity [9]. Within the past decade, consecutive severe flood events occurred in Sri Lanka, and the Colombo District was extremely impacted by these unexpected floods, leading to considerable property and life losses [10]. Statistically, in the Colombo District alone, 1.52 million people were impacted by floods between 1980 and 2019, where 52.75 % of these floods occurred within the past decade [10]. Further, in 2023, Auckland, New Zealand, also faced two catastrophic flood events of unprecedented levels as a result of Auckland Anniversary Day storms and ex-Tropical Cyclone Gabrielle, increasing the damage values ten (10) folds compared to previous flood events, and they were recorded as 200-year return period (RP) events [11].

Evidence from these extremely destructive events attracts global attention towards the need to address the prevailing gap to safeguard built environments and human beings, surpassing complex geographical and hydrological conditions in urban environments [12]. Damage estimations due to flooding should be calculated in monetary terms to have a holistic view of flood damage. It can be executed utilising vulnerability curves developed for the area [13]. Based on damage estimations and urban flood assessments (UFA), innovative strategies and frameworks should be formulated under urban flood risk mitigation [14]. These assessments include both qualitative and quantitative methodologies, aiming to accomplish the primary objective of identifying and analysing the current perceptions of flood risk while generating future flood risk data [15]. Hazard maps generated utilising various satellite data and GIS techniques [16], were used in formulating effective strategies to enhance resilience and mitigate the effects of floods [15]. Resilience is a term that is continuously evolving as the central theory in many study areas. It refers to a system's inherent capability and characteristics to withstand a disturbance and to establish a rapid recovery process [17–20]. Urban environments, including infrastructure, should possess the capability of resisting the risk challenges by transferring to active resilience rather than traditional passive risk control techniques [17, 18]. Thus, the construction of effective Flood Mitigation Measures (FMMs) will act as a major solution for improving active resilience in flood-susceptible cities.

Similarly, a significant amount of research work has been conducted on flood modelling (FM), where FM is essential to understand the flood risk and simulate flood conditions [21] under changing topographical and hydrological conditions. Improving flood mitigation plans in ensuring better risk management includes the establishment of both structural and non-structural FMM [22]. Thus, accurate flood simulations enable the design of systematic structural and non-structural strategies in flood mitigation and management [23] within flood-prone areas, which will increase the flood resilience of urban cities. Common structural FMM includes dam breaching control, canal improvements, the establishment of pumping stations, and river channel clearing, while non-structural measures include warnings, evacuations, and reservoir regulation [22]. Several studies have explored mitigation strategies and structural vulnerability, particularly in both coastal and urban environments. The Florida Public Flood Loss Model (FPHLM) [24] predicts aggregated insured losses combining a hazard model, vulnerability model, and an actuarial model. The workflow of the model moves from the identification of hazard intensities and their conversion to insured losses and damage ratios at the final stages [25]. In the study [26], the FPHLM hazard model is utilised in identifying building damages in coastal areas at different flood wave scenarios compared with the Hazards U.S. Multi-Hazard (HAZUS-MH) model. The Florida Commission on Hurricane Loss Projection Methodology (FCHLPM) is another approach that is used to generate reliable projections of hurricane losses and flood losses in residential properties. Despite these studies, comprehensive evaluations integrating hazard mapping, evaluation of flood damages, and inundation depths connecting with FMMs, to check their efficacy were very limited, and that gap was aimed to be filled within the study.

As mentioned, a significant number of studies have focused on individual aspects of flood risk, such as hazard mapping, hydraulic modelling, or economic damage assessments, but there is a lack of integrated frameworks combining above mentioned individual aspects, that evaluate the combined physical and financial benefits of FMMs. Addressing this gap, the study presents a novel methodology that links flood hazard mapping, hydrodynamic modeling using Hydrologic Modelling System (HEC-HMS V4.12) and River Analysis System (HEC-RAS V6.6) software, and vulnerability-based flood damage estimations. Furthermore, as a unique aspect of the study, it incorporates an investment viability analysis to provide a financial justification of implemented FMMs.

As an application of the methodology, two hazard assessments were conducted for two case study areas, Colombo, Sri Lanka, and Auckland, New Zealand. These assessments were performed utilising ArcGIS Pro V3.3 software (ESRI, USA), considering Elevation, Slope, Land use (LULC) patterns, Drainage Density, Proximity to River, Soil type, and Rainfall as flood susceptibility factors within the considered urban environments. For Colombo, flood inundation maps were generated for "without FMM" and "with FMM" scenarios, to evaluate the effect of FMM in flood inundation depth and extent reduction. It was conducted and presented as a pilot study for Madiwela South diversion, utilising the Hydrologic Engineering Centers (USACE, USA) hydrologic/hydrodynamic model combination with HEC-HMS V4.12 and HEC-RAS V6.6 software. The resulting flood depths and extents were used to estimate tangible and intangible damages under varying return periods through vulnerability curves. The calculated values were used to evaluate the economic soundness of nine (9) FMMs implemented by the Sri Lanka Land Development Cooperation (SLLDC) in the Colombo Metropolitan Area, Sri Lanka. This study was conducted for the selected areas and FMMs as a preliminary application, and it can be applied for any global scenario to reveal insights into the effect of urban floods, as well as to assess the suitability of proposed FMMs in considered study areas, focusing on their efficiency in flood damage reductionThis addresses the critical gap created by the lack of a well-structured methodology for assessing FMMs, thereby supporting the decision-making process in achieving urban flood resilience.

2. Materials and methods

2.1. Case study area 1 – Colombo metropolitan area, Sri Lanka

Colombo Metropolitan Area extends from latitude 6° 43' 00″ N to 6° 58' 00″ N and longitude 79° 50' 00″ E to 80° 00' 00″ E, and a part of the research area belongs to the downstream of Kelani River Basin, which is the fourth largest in Sri Lanka with a varying annual rainfall of 2,500 mm to 5,500 mm. Out of the total land extent covering Divisional Secretarial Divisions (DSDs) of Colombo, Thimbirigasyaya, Dehiwala, Moratuwa, Kesbawa, Rathmalana, Maharagama, Kaduwela, and Kotte of 27,165 ha is shown in Fig. 1.

These areas experience rains mainly due to the South-Western monsoon from May to September and inter-monsoons from March to April and October to November. Both authorised and unauthorised development initiatives, waste dumping to canals, backwater effects, irregular canal maintenance, and wetland filling result in an increase in hindered infiltration and disruptions to the natural and man-made drainage and runoff paths, leading to flow stagnation and accumulation in low-lying surfaces. Furthermore, being downstream of the Kelani River basin, the northern part of the research area is also subjected to riverine flooding caused by heavy precipitation events in the upstream, increasing the tendency of getting flooded. Due to these scenarios, the ability to resist higher precipitation events within the study area is

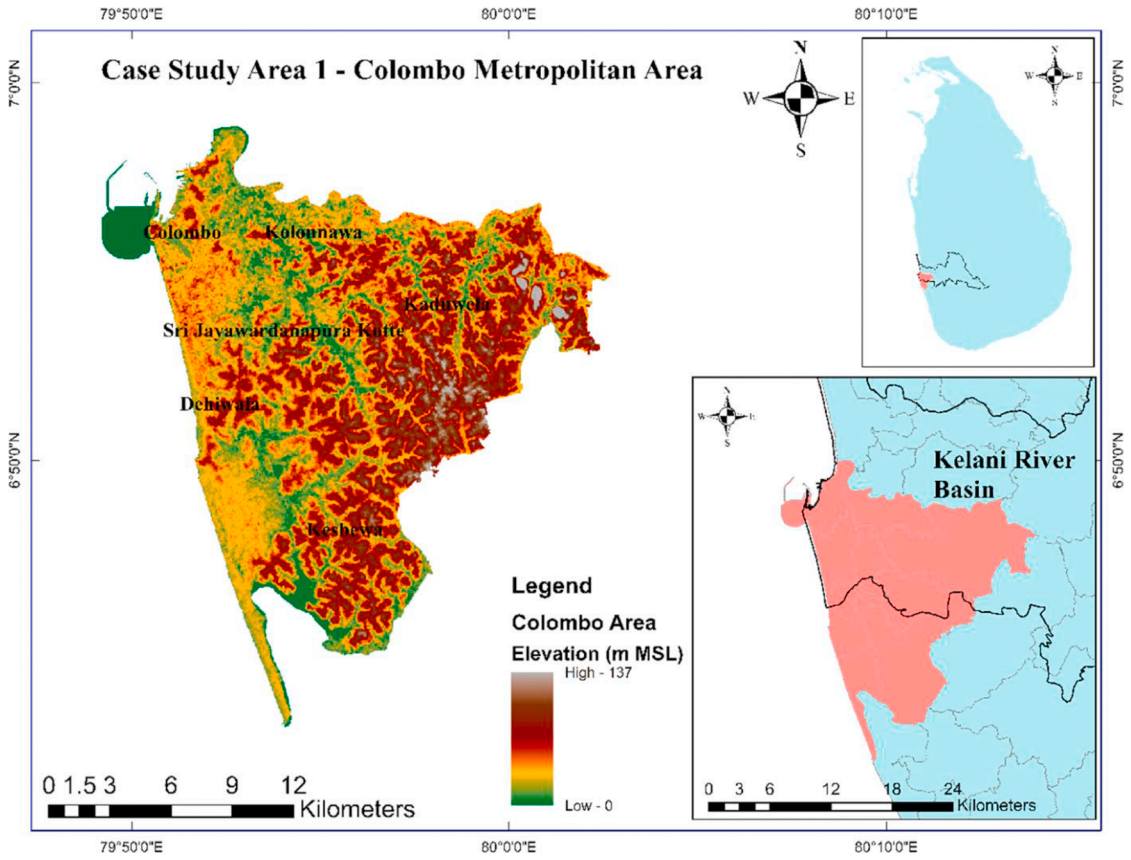

Fig. 1. Case study area 01: Colombo metropolitan area, Sri Lanka, used for flood hazard mapping.

reduced, leading to frequent flood events.

2.2. Case study area 2 – Auckland, New Zealand

Auckland, New Zealand, situated between latitude 36° 50' 00″ S and 37° 05' 00″ S and longitude 174°35' 00″ E and 174° 50' 00″ E (Fig. 2), covers a significant area, including the central business district and surrounding suburbs of New Zealand. This region experiences a temperate maritime climate with relatively mild temperatures year-round. Auckland's rainfall is distributed fairly evenly throughout the year, with an average annual precipitation of approximately 1,300 mm. The city's climate is influenced by its proximity to the Tasman Sea and the Pacific Ocean, leading to moderate rainfall and occasional heavy downpours. In January 2023, Auckland faced severe flooding due to intense and persistent rainfall from ex-Cyclone Hale, which led to widespread damage, including road closures and property damage.

2.3. Methodology

The overall methodology of the study is illustrated in Fig. 3 and is composed of 4 sub-studies to generate a comparison between the "with FMM" and "without FMM" scenarios under different flood inundation depths and flood damage. The methodology is subsequently further extended with an investment viability analysis considering the calculation of the Benefit-to-Cost (B/C) ratio and Net Present Values (NPV) of the currently implemented FMM by SLLDC. The sub-methodologies for hazard assessment, flood-inundation mapping, damage estimations, and investment viability are detailed in the following sections.

2.3.1. Hazard assessment

The study identified the frequently used urban flood susceptibility factors as Slope, Elevation, Proximity to River, LULC, Curvature, Rainfall, Soil Type, Drainage Density, and others [27]. Through an investigative study conducted in two pilot research areas, susceptibility factors leading to increased UFs were identified, and thematic maps were created to represent the influence of each factor using DEMs and other remote sensing data. Table 1 shows data sources and the resolution levels of different data sources that were utilised to generate distinct thematic maps. Normalised weights were allocated to each influential factor, and scores were allocated to sub-classes under each factor depending on their percentage of influence on urban floods. By merging generated thematic maps together, the overall hazard index for the study areas was calculated using Equation 1 [28], based on which the hazard maps were created subsequently, following:

$$\textit{Flood Hazard} = \sum W_i X_i \tag{1}$$

where W_i is the weight of factor i and X_i is the sub-class rating of factor i.

As the next step of the approach, research areas were divided into four (4) zones based on the computed hazard index and maps, each representing different levels of flood risk: extremely high, high, moderate, and low. To assign weights to selected factors, a normalised relative weighting method using an Analytical Hierarchy Process (AHP) pairwise matrix was used. This approach can be utilised to make a series of complex decisions, eliminating biases as it assesses the consistency of results [29]. This process was conducted in a Geographic Information System (GIS) environment with the help of ArcGIS Pro spatial data processing software.

2.3.2. Flood inundation mapping

The flood inundation maps were generated considering two scenarios, "without FMM" and "with FMM", to examine the reductions in flood inundation depths after the implementation of FMMs. As the application, the selected FMM is the Madiwela South Diversion,

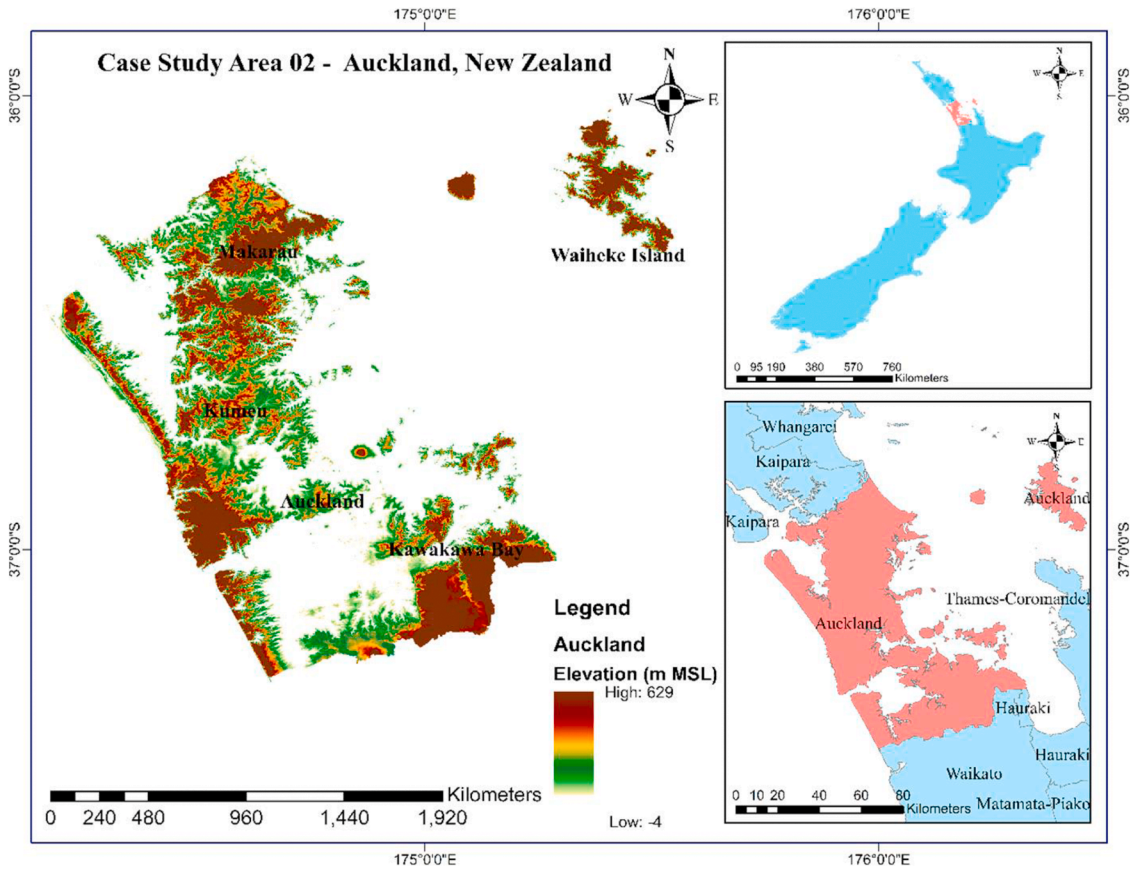

Fig. 2. Case study area 02: Auckland, New Zealand, used for flood hazard mapping.

Colombo, Sri Lanka. The catchment area of the Madiwela South Diversion is the upstream part of Parliament Lake, having an area of 19.32 km^2 within Kotte and Maharagama DSDs (Fig. 4). The catchment was stimulated for precipitation events with different RPs of 2-year, 5-year, 10-year, 25-year, 50-year, and 100-year. The balanced storm data were produced by Intensity-Duration-Frequency (IDF) curves developed for Colombo as described by using HEC-HMS V 4.12 software [30]. The HEC-HMS software is publicly available and was developed by the Hydrologic Engineering Center of the U.S. Army Corps of Engineers. It is a hydrological model that supports both lumped and distributed parameter-based modelling [31] and possesses mathematical models in simulating the precipitation runoff-routing processes of dendritic watershed systems [32]. The basin model, which is a representation of real-world hydrological phenomena of the catchment area, was developed, incorporating the Soil Conservation Service (SCS) curve number method as the loss method, SCS unit hydrograph method as the transform method, recession method as the base flow method, and lag method as the routing method. The HEC-HMS model was calibrated, validated, and applied to generate runoff for the basin.

The HEC-RAS V6.6 software was utilised to determine flood-inundation areas and depths relative to mean sea level (MSL) under both 1D and 2D conditions. HEC-RAS software is a commonly applied open-source software developed by the Hydrologic Engineering Center of the U.S. Army Corps of Engineers [33]. It is used in both commercial and government sectors for flood simulations, flood risk modelling, and predictions [34]. The HEC-HMS model outputs and HEC-RAS models are directly coupled together through standardized Data Storage System (DSS) files [33]. The streamflows generated for different return periods using the validated HEC-HMS model are directly imported to HEC-RAS as inflow hydrographs as upstream boundary conditions for both 1D and 2D unsteady flow simulations. This interoperability enables efficient scenario analysis as the study is conducted for several return periods for the same catchment, where adjustments to rainfall in HEC-HMS are automatically reflected in HEC-RAS simulations without the need for manual data transfer. This makes the application of HEC software particularly advantageous over other modeling approaches like MIKE FLOOD, which are not open-source, with high computational demands and additional integration steps, as it offers a flexible, cost-effective, and reproducible solution for urban flood modeling across different return periods.

To digitise the output data of flood depths and extents and represent the catchment topography, HEC-GeoRAS and RAS Mapper were employed. HEC-GeoRAS, an extension of ArcGIS software, was initially developed through a research collaboration between the Environmental Systems Research Institute (ESRI) and the HEC. This extension permits the creation of engineering data related to rivers, which is subsequently transferred to HEC-RAS. Using this data, HEC-RAS develops a map that displays the speed of water current and flood information within the considered drainage basin [35]. Using the developed models, the “with FMM” and “without FMM” alternative conditions were simulated, and inundation depths were obtained.

Initially, HEC-RAS modelling was conducted for “without FMM” conditions, and flood inundation depths were simulated for a 1D/2D unsteady flow environment. For 2D simulations, initially, a 2D computation mesh was generated, with a closed polygon having computation cells inside the domain, and for 1D analysis, a cross-section processing was executed. Considering the boundary conditions for both upstream and downstream in the simulations, the flow hydrographs generated using HEC-HMS were imported into HEC-RAS via DSS (Data Storage System) files and applied as upstream boundary conditions, enabling direct and dynamic integration between the two models. For the downstream boundary, normal depth under gravity flow was imposed for both 1D and 2D unsteady flow simulations. The roughness resistivity was estimated based on different land use patterns available within the

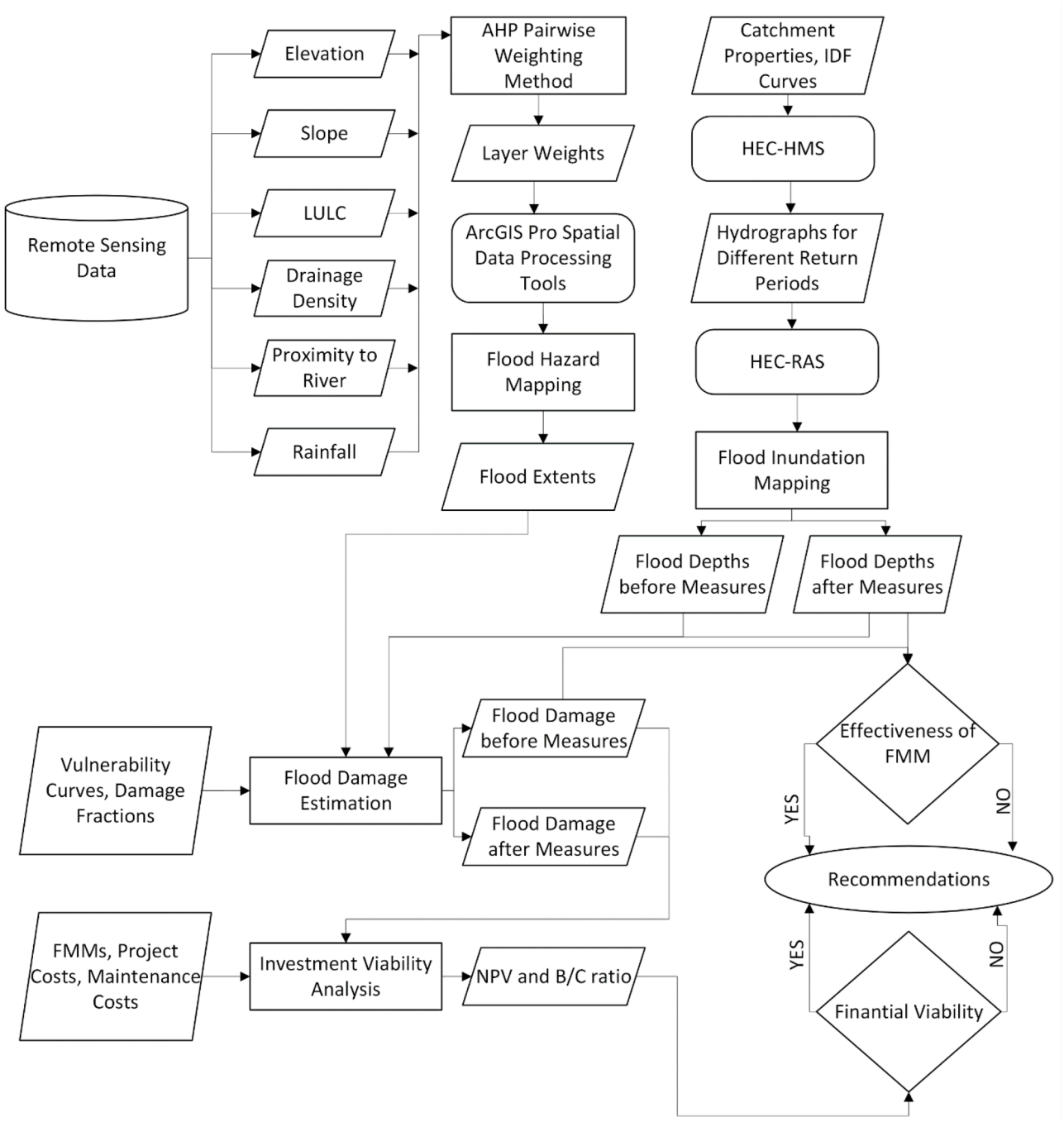

Fig. 3. Methodology flowchart representing the 4 sub-studies (LULC- Land use and land cover, AHP- Analytical hierarchy process, IDF-Intensity-duration-frequency curves, HEC-HMS-Hydraulic engineering center-hydraulic modelling system, HEC-RAS- Hydraulic engineering center-river analysis system, FMM- Flood mitigation measures, NPV- Net present value, B/C- Benefi-to-Cost).

area using Landsat 8 imagery processing and applying ArcGIS Pro software, and Manning's roughness value was calculated. Further, model stability was established using calculated time steps according to the Courant-Friedrichs-Lewy condition. The model was simulated under unsteady flow conditions, and flood inundation depths for each hour were obtained.

In this study, the HEC-HMS model was driven by synthetic rainfall derived from IDF curves for multiple return periods, making traditional calibration against observed streamflow infeasible. To improve model reliability, parameters, including Curve Number (CN), initial abstraction ratio, impervious percentage, lag time, and baseflow recession constant, were adopted considering the comparable urbanized setting and hydrological response characteristics of the Lower Kelani River Basin [31,32]. HEC-RAS calibration was conducted separately for 1D and 2D simulations. For the 1D model, Manning's roughness coefficients (0.035-0.060) were refined based on land use classifications, and a normal depth (0.005) boundary condition was applied using slope values derived from the digital elevation model. The 2D model calibration involved spatially varying roughness assignments, mesh resolutions, and dynamic time step selection based on the Courant-Friedrichs-Lewy condition to ensure numerical stability. Further, model sensitivity was assessed by varying key model parameters within plausible ranges to evaluate their influence on discharge and flood depth. The analysis revealed that outputs were most sensitive to

Table 1
Remote sensing data sources used for flood hazard mapping and resolution levels.

Data Requirements	Source	Resolution Level
Slope and Elevation	USGS Earth Explorer: https://earthexplorer.usgs.gov/ Shuttle Radar Topography Mission (STRM) DEM Data, SRTM 1 Arc-second Global coverage	30-m cell size resolution
Landcover	https://livingatlas.arcgis.com/landcoverexplorer ESRI Sentinel 02 LULC data	10-m cell size resolution
Soil Types	https://www.fao.org/soils-portal/data-hub/soil-maps-and-databases/ Food and Agriculture Organization (FOA)-UNESCO, Digital Soil Map of the World (DSMW), updated in 2023	5-arc minute cell size resolution
Drainage Density	USGS Earth Explorer: https://earthexplorer.usgs.gov/ Landsat 8 collection Level 2 DEM data	80-m cell size resolution

the CN in HEC-HMS and the downstream normal depth boundary condition in HEC-RAS. Given the integrated nature of the HEC-HMS and HEC-RAS modeling framework, system-level validation was performed using simulated flood inundation depths. This approach ensured that the coupled model reliably captured the rainfall-runoff and flow routing processes across the study domain. Validation was conducted for the 50-year RP at the Madiwela South Diversion and cross-compared with MIKE 11 model results currently used by the SLLDC. Objective functions, including Nash–Sutcliffe Efficiency (NSE) and Root Mean Square Error (RMSE), demonstrated strong agreement as in Section 3.2.

2.3.3. Flood damage estimation

This section of the study examines hypothetical damages that could occur due to flood conditions, with rainfall levels with different RPs in monetary terms. The two main (2) factors that were considered under damage calculations were inundation depths and inundation extents; depending on those two prioritized factors, tangible and intangible damages due to flooding were calculated. Damage estimations were calculated for two (2) different scenarios, "without FMMs" and "with FMMs", under RPs of 5-year, 10-year, 20-year, and 50-year for different inundation areas. The two scenarios demonstrate the flood damage before implementing FMMs and after implementing FMMs, which can be utilised to identify the damage reduction after implementing FMMs.

To demonstrate the methodology, the implemented structural FMMs by the Urban Water Management Division of the SLLDC were considered. Those interventions can be summarized under canal improvements, new canal developments, drainage network improvements, pumping station installations, wetland degradation, and some Blue and Green Infrastructures, as in Fig. 5.

Additionally, to increase the accuracy of calculations, damage estimations were further divided into two subclasses: favourable and unfavourable conditions. The favourable condition was considered under low tide levels with less rainfall for the upper catchment area of the Kelani River Basin. Unfavorable conditions were considered vice versa, which led to an additional increase in flood levels in the considered case study area. The inundation data were collected from a previous flood study [36], and the value at risk was extracted from the other available sources [37], for Western Province, Sri Lanka. To calculate damages, the main damage categories were selected as residential buildings, warehouses, industrial buildings, offices, shops, schools, hospitals, other infrastructure, and vehicles. They were selected based on a detailed assessment of the Colombo study area to ensure

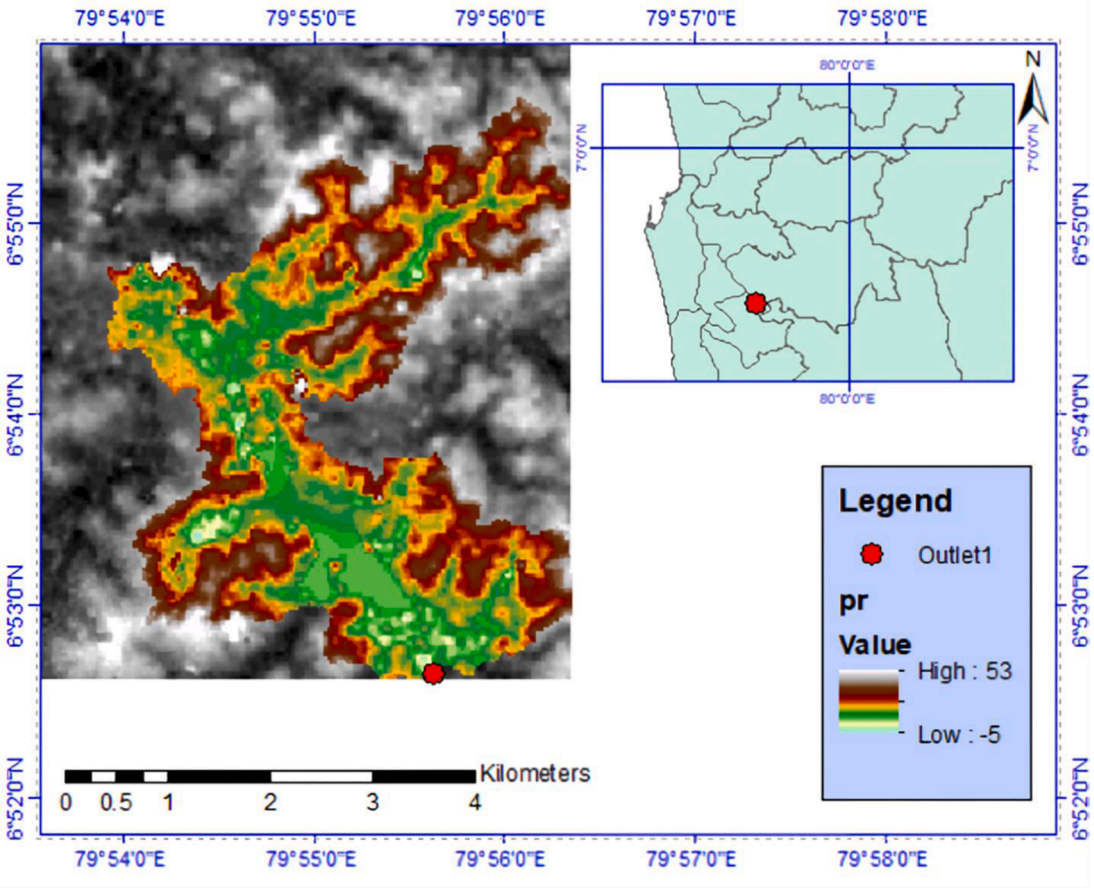

Fig. 4. Catchment for Madiwela South Diversion, Colombo, Sri Lanka, used for flood inundation mapping using HEC-RAS as a case study.

Fig. 5. Structural interventions implemented by SLLDC as flood mitigation measures at Colombo, Sri Lanka (a) St. Sebastian Canal (b) Madiwela East Diversion (c) Pumping station at unity place (Images from Urban Water Center, SLLDC).

comprehensive representation of the built environment and critical assets exposed to flood risk. Buildings were categorized under Single-storeyed and Two-storeyed, accounting for both content damage and structural damage. Damage fractions were extracted from generated flood vulnerability curves (Fig. 6) for Colombo, Sri Lanka, under varying inundation depths as in [38]. Vulnerability curves are empirical models derived from post-disaster damage assessments, insurance claims, engineering models, or a combination of these three [25]. These vulnerability curves, which were developed for Colombo, enable the ability to execute accurate damage estimations by capturing the unique structural, socio-economic, and land-use characteristics present within the catchment. The localized calibration enhances the reliability of depth-damage relationships compared to generalized or globally derived functions, thereby improving the relevance and precision of the economic loss assessment. Further, to incorporate damages to intangible assets and economic losses, a multiplication factor of 1.5 [39] was used to adjust the estimated damage. Vilier [40] introduced an additional 0.25 factor to capture business interruption as an indirect damage, but did not consider human damage (fatalities). Further, a cost–benefit analysis conducted specifically for the Colombo metropolitan area applied a range of multiplication factors from 1.1 to 1.5 for indirect losses. Given the urban morphology of Colombo, characterized by relatively shallow inundation depths, flat terrain, and dense population clusters, flood-related fatalities are considered negligible, yet the socio-economic disruptions remain significant [39]. Thus, the use of the 1.5 multiplier reflects an upper-bound yet contextually appropriate estimate that encompasses both direct damages and broader non-structural impacts relevant to frequent urban flood events. The damage values were estimated using Eq. (2) as per [39].

$$Flood\ Damage = \sum_{i=1}^{m} S_i \sum_{i=1}^{n} f_{ij}(d_i) n_{ij} \tag{2}$$

In the equation, S_i is the value of the risk, where i refers to different main damage categories as mentioned, $f_{ij}(d_i)$ is the damage fraction for

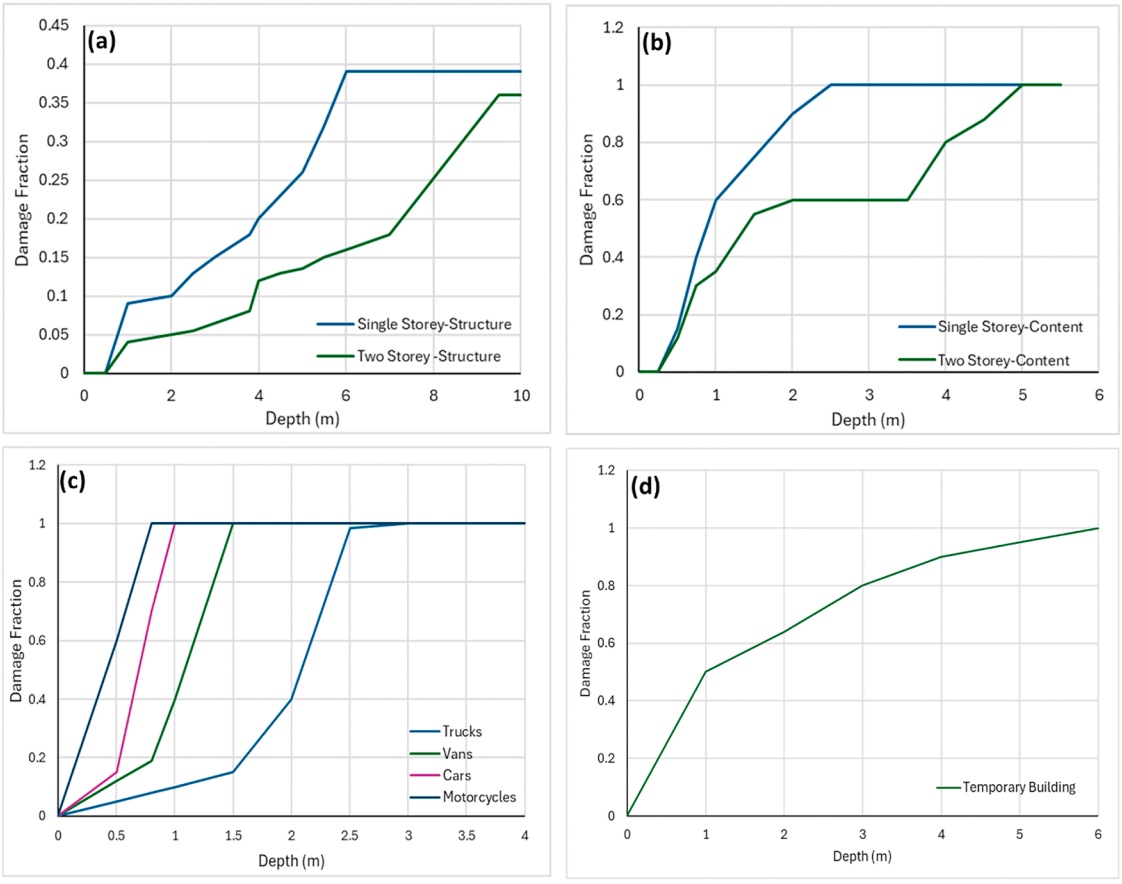

Fig. 6. Vulnerability curves for Colombo, Sri Lanka (a) building structure damage curve (b) building content damage curve (c) vehicle damage curve (d) temporary structures damage curve [38].

various elements (j) under main damage categories [35], and n_{ij} is the elements at risk. A main damage category was subdivided into several elements to increase the accuracy in allocating acceptable damage fractions. For example, residential buildings were subdivided as: Temporary structure (structural damage), Temporary structure (content damage), Single-storey structure (structural damage), Single-storey structure (content damage), Two-storey structure (structural damage), and Two-storey structure (content damage). Similarly, all nine (9) main damage categories were subdivided to generate fifty (50) elements, and those were allocated with damage fractions considering the flood inundation depths utilizing vulnerability curves as per Fig. 6. The calculated flood damages were utilized to calculate the annual estimated flood damages (EAD) from Eq. (3) [39], considering different RPs, having p as the exceedance probability (1/T) and p_{max} as the largest exceedance probability.

$$EAD = \int_0^{p_{max}} Damage(p)dp \tag{3}$$

These equations were numerically solved to estimate the flood damage at different RPs for corresponding inundation depths. The inundation depths were based on past flood occurrences in the research area. The same procedure was applied under the "with FMMs", and the damage values were calculated. A comparison of two scenarios was undertaken to evaluate the effects of flood mitigation measures on damage reduction.

2.3.4. Investment viability analysis

As the final sub-study of the main study, an investment viability analysis was conducted to identify another criterion to check the effectiveness of the considered FMMs. The projects that the SLLDC has already implemented from 2000 to 2022 for flood mitigation in the Colombo Metropolitan Area were considered, and project cost data and project maintenance cost data were collected from the SLLDC. In calculating the benefit of FMMs, a 50-year RP event was considered. Flood damage was calculated utilizing Eqs. (2) and (3) as in Section 2.3.3. for "with FMMs" and "without FMMs", and the difference in the damage was considered as the acquired benefit from the considered FMM [41]. Nine (9) FMMs were considered in the study, and the reduction of flood damage was calculated for each FMM in monetary terms, individually considering the flood inundation depths for a 50-year return period flood under "without FMM" and "with FMM" scenarios. Integrating project cost, maintenance cost, and project benefit, the B/C ratio for the project's Net Present Value (NPV) was calculated utilizing Eqs. (4) and (5) as in [42]:

$$NPV_{ps} = PV(B_{ps}) - PV(C_{ps}) = \sum_{t=1}^{T} \frac{(\propto EADr_{t,ps})}{(1+r)^t} - \left(\sum_{t=1}^{T} \frac{(M_{t,ps})}{(1+r)^t} + I_{0,ps} \right) \tag{4}$$

$$\frac{B}{C}Ratio_{ps} = \frac{\sum_{t=1}^{T} \frac{(\propto EADr_{t,ps})}{(1+r)^t}}{\sum_{t=1}^{T} \frac{(M_{t,ps})}{(1+r)^t} + I_{0,ps}} \tag{5}$$

where, NPV_{ps} is the net present value of the protection standard, which refers to the considered structural FMMs, $PV(B_{ps})$ is the present value of the benefit achieved through implementing those measures, and $PV(C_{ps})$ is the present value of the project cost. The multiplication factor ($\alpha = 1.5$) is used to account for the damage caused to intangible assets, $ESDr_{t,ps}$ is the estimated annual damage for each year throughout the project's lifetime, $M_{t,ps}$ is the maintenance cost for T years, and $I_{0,ps}$ is the investment cost for the protection standard. A lifespan (T) of 30 years was considered as the project life as per SLLDC project reports, r is the discount rate (10 %) along with value depreciation at a rate of 6 %. Benefits acquired from each FMM were represented by the sum of the EAD, for each time-step t, over the total lifespan of 30 years. Considering the time value of money, with the changes in the economic value of the country, the acquired benefit values were accounted for a 6 % increment for each year relative to the economic regression in Sri Lanka. Under this criterion, a higher NPV and B/C ratio indicate a greater financial viability and profitability of the investments. A higher NPV suggests that the expected benefit of FMMs has exceeded the initial and ongoing maintenance costs, making it a financially attractive option. Similarly, a higher B/C ratio, which represents the proportions of benefit over costs, indicates that flood mitigation projects yield substantial returns relative to the project's initial and maintenance costs. Thus, using these two indicators, a more economical FMM can be justified.

3. Results and discussion

3.1. Hazard mapping

Hazard Mapping for Colombo, Sri Lanka, and Auckland, New Zealand, was conducted to identify the factors that increase the hazardous nature within the study areas as mentioned in the pairwise comparison matrix methodology, utilising AHP. Each developed thematic map layer, such as elevation, slope, LULC, proximity to rivers, drainage density, rainfall, and soil type, was given a normalised weight, and by merging all the weights using ArcGIS Pro (V3.3) software, flood hazard maps were developed for both the study areas to identify the most hazardous locations. Fig. 7 shows the hazard map for Colombo, Sri Lanka.

To generate the multi-criteria analysis, factors were allocated with normalised weights considering their level of influence through an AHP pairwise comparison matrix, and sub-classes were allocated with susceptibility sub-class ratings (SR). Using the created thematic maps, the influence of each factor in increasing flood susceptibility at different sub-classes was checked. Considering elevation, the total research area was divided into 4 sub-classes: 0–5 m, 5–10 m, 10–20 m, and above 20 m. In general, 36 % of the area falls in the range between 0–5 m and 20 % of the area within 5–10 m, showing low elevation conditions. Similarly, a slope analysis for the area was conducted considering 4 sub-classes, and the area showed a predominantly flat terrain leading to very mild slopes, with 82 % of the area having a slope of 0°-5°. Both factors of low elevation and having a mild slope within the case study area restrict the gravity flow, prompting surface flow accumulations leading to flooding. Thus, under the AHP analysis, when allocating SR for factors of elevation and slope, lower values were given a higher rating of five (5) or four (4), and higher values were given a lower rating of two (2) or one (1). The LULC was identified as another main influencing factor that increases flood susceptibility. The total research area was classified under 5 sub-classes: water bodies, built-up areas, agricultural areas, trees or bare lands, and wetlands. From the thematic map for LULC, 85.6 % was identified as built-up areas, converting pervious surfaces to impervious, reducing infiltration ability. Thus, a higher SR was given to water bodies and built-up areas, and the lowest to wetlands, as they contribute as retention ponds for flooding. Drainage Density within the area was classified as moderate, having a value range from 0.03–0.14 km/km^2, showing a moderate runoff potential. Considering the Proximity to River, the northern part of the case study area shows a very close proximity to the Kelani River. To identify mostly affected areas, the total case study area was classified under the main 4 buffer zones, as 0–200 m, 200–500 m, 500–750 m and above 750 m, and SRs were given from the lowest buffer to highest buffer as highest value to lowest value, considering the ability to undergo a flood condition, 8 % of the area was identified within the range of 0–200 m and 12.3 % in 200–500 m. Further, soil type was also considered an influential factor due to the variation of infiltration ability with the type of soil. The classification was executed under five (5) soil types. Still, only two (2) main soil types were found in the case study area as red-yellow podzolic soils (63.2 %) with either soft or hard laterite and the rest as alluvial soils. Considering the rainfall conditions, five (5) main precipitation sub-classes were created and allocated with SR, as very heavy rain (>100

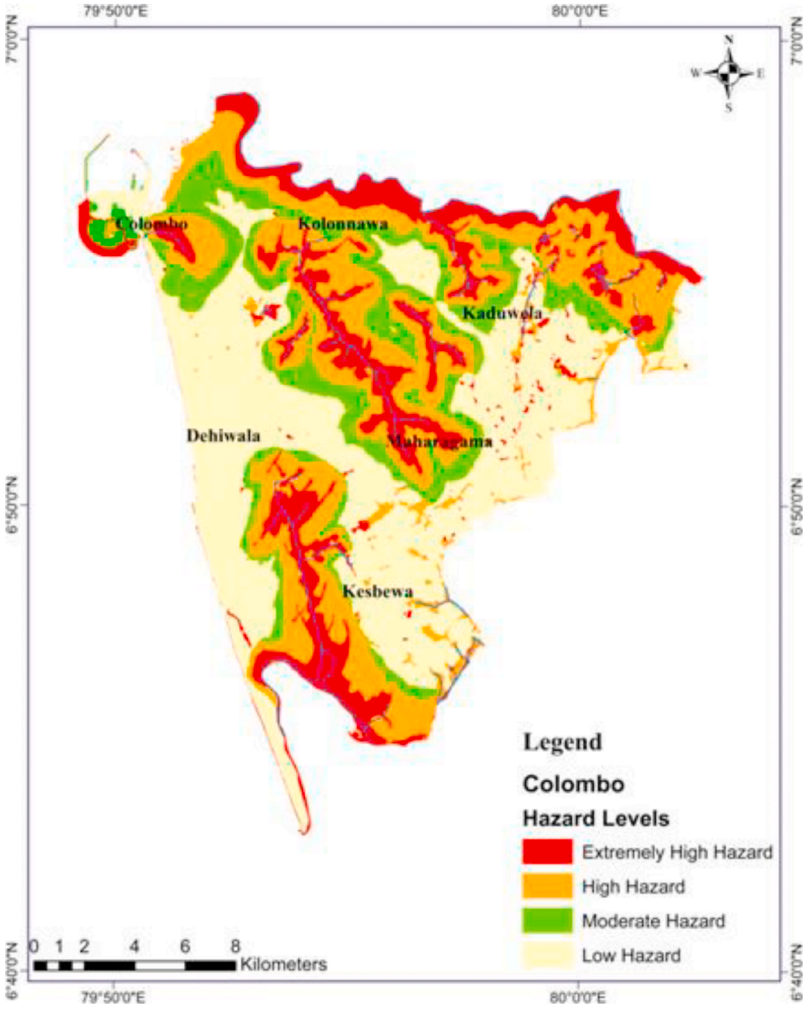

Fig. 7. Hazard map for Colombo Metropolitan Area, graded from extremely high to low hazard; A higher flood risk is concentrated in areas of Kolonnawa, Kaduwela, and Kesbewa.

mm/day), heavy rain (50–100 mm/day), moderate rain (20–50 mm/day), light rain (5–20 mm/day) and very light rain (< 5 mm/day). It was identified that in the months of May to September, the research area experiences high or extremely high precipitation events, while for other months of the year, precipitation events lie mostly within the range of 20–50 mm/day. Thus, several precipitation events were considered. Utilising normalised weights and SR, normalised sub-class weights were calculated, and Eq. (6) was generated to identify the flood hazard in the research area based on Eq. (1).

$$\textit{Flood hazard} = 0.325 \times (\textit{Slope}) + 0.26 \times (\textit{Elevation}) + 0.158 \times (\textit{LULC}) + 0.131 \times (\textit{Proximity to River}) + 0.042 \times (\textit{Drainage Density}) + 0.075 \times (\textit{Rainfall}) + 0.028 \times (\textit{Soil Type}) \quad (6)$$

Considering the Sri Lankan condition, when the rainfall exceeded 100 mm/day, the percentage of moderate hazard area was 47.55 %, and the high hazard area was 11.36 %. This indicates that, during higher precipitation events, more than 50 % of the total research area has a probability of undergoing flooding. Common features that were investigated as reasons for having a high flood hazard level were high built-up area density, low proximity to the Kelani River, and having a land slope of less than 5°. An increase in built-up area density will reduce the infiltration ability and increase the flow accumulations, and a reduced slope will affect the speed of runoff; a reduced slope will minimise flow velocities and increase flow accumulations.

Having a low proximity to the Kelani River directly influences flood occurrences. Thus, areas near the Kelani River undergo riverine floods with the increased water levels in the river. Further, it was seen that Colombo, Kaduwela, Kolonnawa, and Kesbawa DSDs are the most hazardous DSDs due to flooding, and this can be justified through the number of flood occurrences in the past decade according to census report by the Department of Census and Statistics, Sri Lanka, where those DSDs faced 30, 30, 40, 42 floods respectively. Similarly, a study [10] had shown that the highest economic damages and loss of life were found in Kolonnawa and Kaduwela DSDs from past flood events like the 2016 Colombo Floods. Further, generated hazard maps showing the areas with different hazard levels can be utilised to identify the areas that should be given higher attention when structural or non-structural FMMsare implemented.

Similarly, hazard mapping (Fig. 8) was conducted for Auckland, New Zealand, and divided the whole area into 4 main hazard classes: safe, low hazard, moderate hazard, and high hazard. From the generated thematic maps, it was identified that the elevation of the area shows a considerable variation from 0 m to 750 m due to mountainous features, but the Auckland city limits are within the elevation range of 15 m to 35 m, allowing the flow towards the city from elevated locations.

Considering the height ranges, the area was divided into 5 sub-classes as 0–20 m, 20–40 m, 40–60 m, 60–100 m, and above 100 m to allocate SR, and these divisions were created considering the most affected areas in the 2023 Auckland flood conditions. Similarly, slope analysis was also conducted focusing on 4 sub-classes and found that 28.6 % of the total land area was in the slope range of 0°-15°, which was

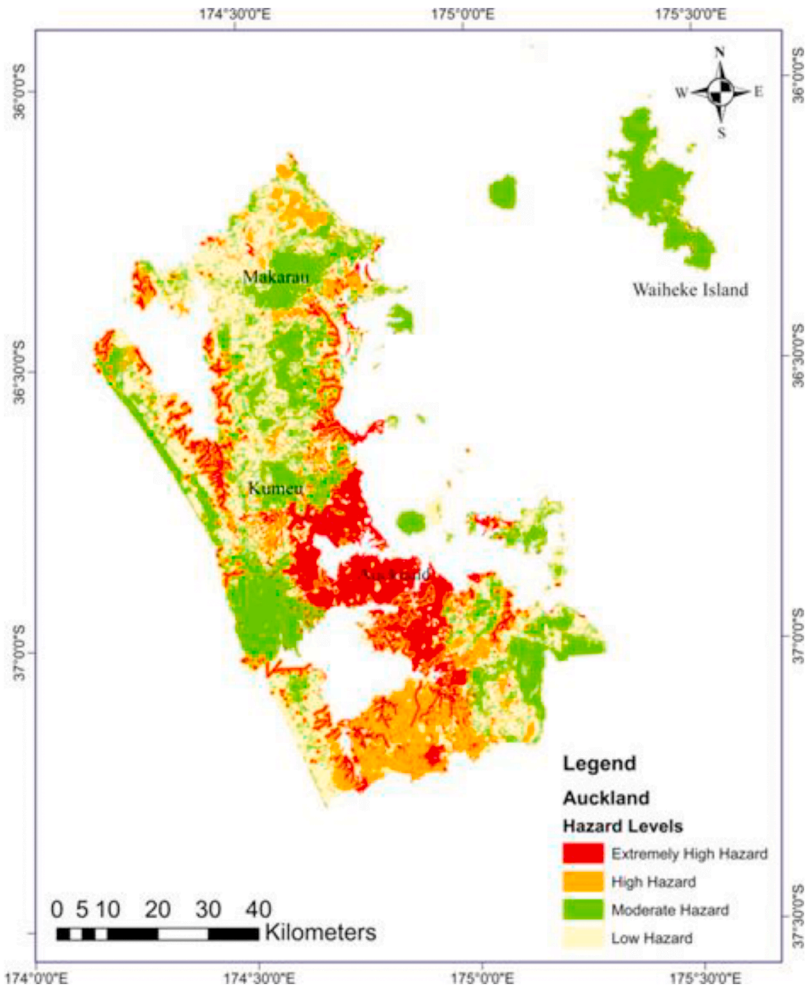

Fig. 8. Flood hazard map for Auckland, New Zealand, graded from extremely high to low hazard; a higher flood risk is concentrated in the Auckland city area.

allocated with the highest SR due to increased flow retentions. Further, hilly areas within the research area had a steep topography of slope 45°-60°, resulting in a higher surface flow towards the mild-sloped city area, leading to pluvial floods. Considering the LULC, the classification was conducted similarly as in case study 01, and 21 % of the total land extent was identified as a built-up area, highlighting higher built-up area density in Auckland city limits. Then, considering the Drainage Density, 56 % of the area fell under 0.04–0.08 km/km^2, having a low Drainage Density value, highlighting its reduced influence in Auckland flooding. Correspondingly, Proximity to River and Soil Type maps were also generated, and SR was allocated. In generating the Proximity to River map, the approach under case study 01 was used to identify the buffer zones and identified that 16 % of the area lies in the range of 0–200 m, showing higher susceptibility to flooding. Similarly, utilising normalised weights and allocated SR, normalised sub-class weights were calculated, and Eq. (7) was generated to identify the flood hazard in Auckland, New Zealand.

$$\textit{Flood hazard} = 0.238 \times (\textit{Slope}) + 0.246 \times (\textit{LULC}) + 0.218 \times (\textit{Elevation}) + 0.182 \times (\textit{Proximity to River}) + 0.095 \times (\textit{Rainfall}) + 0.012 \times (\textit{Drainage Density}) + 0.01 \times (\textit{Soil Type}) \quad (7)$$

The hazard extents were as in Fig. 8, and the percentage extents of the hazard classifications are 22 %, 17 %, 36 %, and 25 %, respectively, for extremely high, high, moderate, and low. From the analysis, it was identified that the Auckland city area has a high hazard level compared to other areas in the region. The main reasons for having high hazard levels in the city area can be justified by the higher built-up area density reducing infiltration, proximity to several river networks, and low elevation and slope within the region, allowing all runoff volume to drain towards the city, similar to the 2023 Auckland floods.

As an expansion of the study, this approach can be applied for similar hazard map generation to other cities that are facing substantial flood risks, like Mumbai in India, Jakarta in Indonesia, and Barcelona in Spain. These cities share common flood-susceptibility characteristics, including a high density of built-up areas, proximity to rivers or coastal areas, and variations in slope and elevations, causing flow accumulations and reducing infiltration abilities. Changes in climate conditions resulting in unexpected precipitation levels have aggravated flood occurrences in terms of both the means of extent and frequency. Thus, by applying similar multi-criteria hazard mapping, city planners can identify the critical spatial extents of urban flooding.

3.2. Flood inundation mapping

Using the HEC-RAS software and RAS Mapper, inundation depths with respect to mean sea level (MSL) and inundation extents were generated for different RPs. To increase the accuracy of the analysis, specific locations were defined using profile lines (PL) to measure flood depths. Four (04) main PLs were utilised: Parliament Bridge, Ethul Kotte Bridge, Kimbulawala Bridge, and profile line 4 in between Parliament Bridge and the Ethul Kotte Bridge, and the length values along the profile lines were used, starting from the right to determine the change of inundation depths along profile lines. The generated 1D and 2D flood maps were presented in Figs. 9 and 10, and inundation depths at

different locations were represented in Table 2.

Initially, HEC-RAS modelling was conducted for "without FMM" conditions, and flood inundation depths were simulated for a 1D/2D unsteady flow environment. For both stimulations, the Saint Venant equation was utilised. Table 2 shows the flood inundation depths under the initial condition, where results for 25-year, 50-year, and 100-year RPs were presented in Table 2 as inundation depths are comparatively negligible for 2-year, 5-year, and 10-year RPs.

The calculated inundation depths have increased with the increase of the RP. The generated model was validated using the model results for Colombo, Sri Lanka, using the MIKE 11 model by [37], which is the currently used model for flood simulations at SLLDC. The deviations of depths were calculated using objective functions, Relative Root Mean Square Error (RRMSE), N-S Coefficient Efficiency (EF), and Coefficient of Determination (CD). The error calculations predict that 2D analysis results were more accurate compared to 1D simulations.

In the 2D analysis, the RRMSE value was 0.34, suggesting a minor model error compared to the variability in the MIKE 11 model data rather than the 1D model (RRMSE-0.42). Similarly, the Nash Coefficient (NSE) was higher in the 2D model (0.78), indicating a relatively good agreement between the predicted and observed values compared to the 1D model (with a NSE of 0.64), with higher NSE values suggesting better model performance.

Thus, better performance of both 1D and 2D models can be concluded with the error ranges, compared to the MIKE 11 model, but the 2D HEC-RAS model shows a higher rate of agreement compared to the 1D model. Consequently, the validated model was applied to simulate the "with FMM" scenario for the Madiwela South Diversion, which carries a discharge capacity of 40 m^3/s. The scenario was modelled for 25-year and 50-year RPs, and results were compared with the previous "without FMM" scenario, and inundation depth reductions were experienced, as in Table 3. To simulate the scenario, a fixed outflow of 40 m^3/s was given as the downstream boundary condition for the model.

From model simulations for "with FMM", a clear reduction of the inundation depths was seen after the implementation of the diversion at all the considered inspection locations. Flood inundation depth for a 50-year RP rainfall, at a 750 m location point, in the Parliament Bridge was derived as 2.26 m at "with FMM"; subsequently, after the implementation of the FMM, the depth was reduced to 1.99 m, showing a percentage reduction of 11.9 %. Thus, the effect of FMM in the reduction of flood inundation depths can be justified using the applied approach, and this study can be taken as a preliminary approach to the methodology that can be applied in more complex situations and also to stimulate the effects of FMMs at the planning stages. Reductions in flood-inundation depths directly translate to property damage reductions, reducing recovery costs and enhancing city resilience. Through the application of flood-inundation mapping using HEC-RAS software, city planners can make data-driven decisions by identifying the best and most effective FMM to be implemented at the regional level.

3.3. Flood damage estimations

The damage estimations were calculated according to the inundation

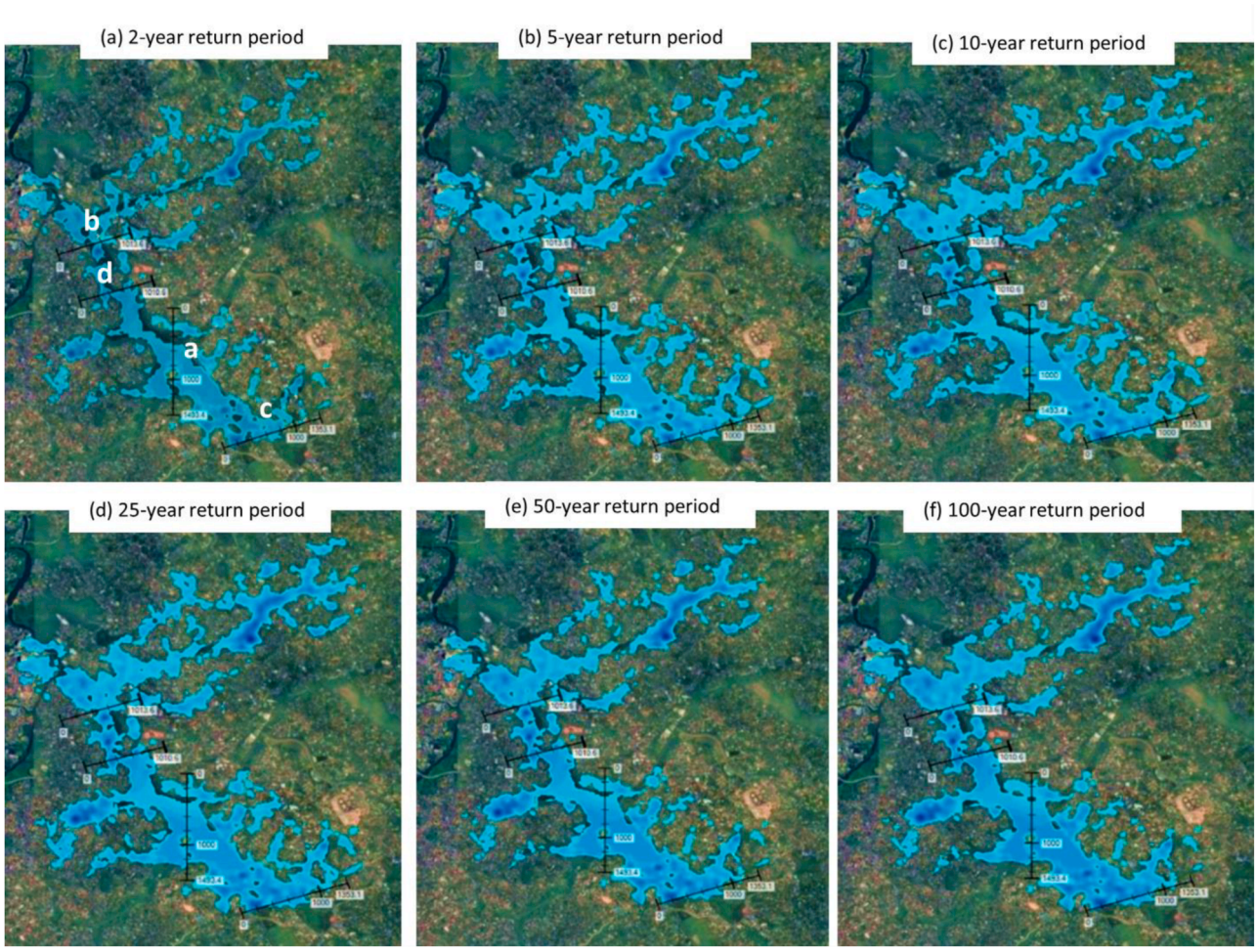

Fig. 9. 2D flood inundation mapping, (a)- Parliament Bridge (b)- Ethul Kotte Bridge (c)- Kimbulawa Bridge (d)-Profile Line 4 (PL4)(Profile lines are marked in black as mentioned in Table 2, and blue extent shows flood inundation extents the gradient of the colour code of shows increase of flood depths).

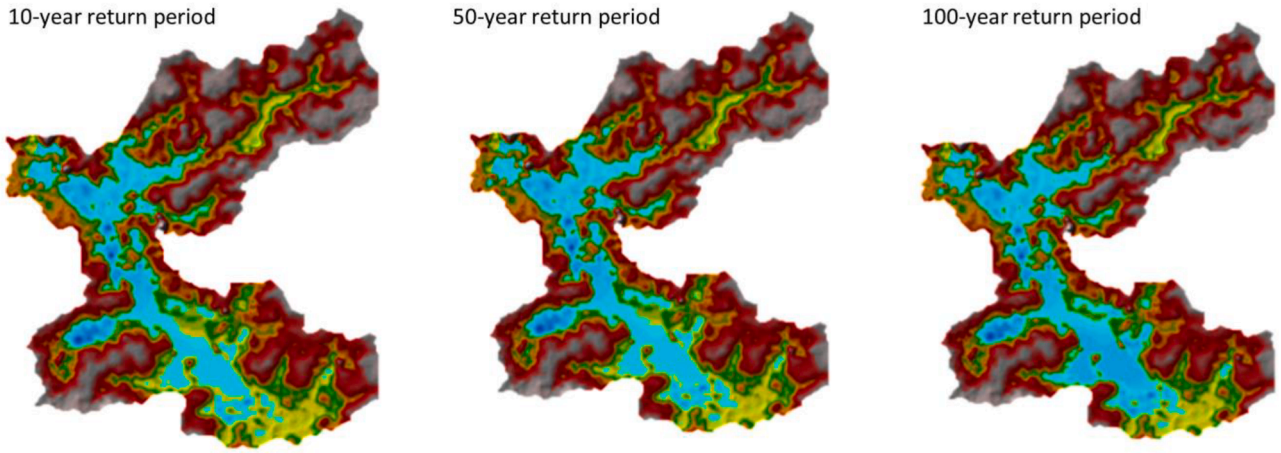

Fig. 10. 1D flood inundation mapping catchment of Madiwela south diversion for 10-year, 50-year and 100-year return period floods (the blue extent shows flood inundation extents, and the colour gradient of the color code shows increase of flood depths).

Table 2
Flood inundation depths (in m) at inspection points along the profile lines for "without FMM" scenario in Madiwela South diversion, Colombo, Sri Lanka.

25-year Return Period								
Profile Lines to Measure Flood Depths	250 m		500 m		750 m		1000 m	
	1D	2D	1D	2D	1D	2D	1D	2D
Parliament Bridge	0.17	0.64	0	0.79	1.86	2.43	0.63	2.17
Ethul Kotte Bridge	0.34	0.00	1.68	0.75	0.86	1.76	0.00	1.40
Kimbulawala Bridge	0.00	5.95	0.00	3.22	0.00	2.94	0.00	0.00
Profile Line (PL) 4	0.00	1.13	2.51	1.49	0.00	0.12	0.00	0.00
50-year Return Period								
Profile Lines to Measure Flood Depths	250 m		500 m		750 m		1000 m	
	1D	2D	1D	2D	1D	2D	1D	2D
Parliament Bridge	0.17	0.85	0.00	1.17	2.26	2.75	2.26	2.05
Ethul Kotte Bridge	0.24	0.00	1.68	0.89	0.86	0.80	0.86	0.30
Kimbulawala Bridge	0.00	5.45	0.00	3.54	0.00	3.41	0.00	0.00
Profile Line (PL) 4	0.00	0.00	2.51	1.23	0.00	0.00	0.00	0.00
100-year Return Period								
Profile Lines to Measure Flood Depths	250 m		500 m		750 m		1000 m	
	1D	2D	1D	2D	1D	2D	1D	2D
Parliament Bridge	0.23	1.16	1.01	1.38	2.45	3.54	1.92	1.63
Ethul Kotte Bridge	0.00	0.00	1.28	1.19	0.59	0.98	0.00	0.85
Kimbulawala Bridge	0.00	6.35	0.00	3.93	0.00	3.67	0.00	0.00
Profile Line (PL) 4	1.42	0.00	2.01	1.67	0.00	0.64	0.00	0.00

Table 3
Flood inundation depths (in m) at 50-year return period along the profile lines for "with FMM" scenario in Madiwela South diversion, Colombo, Sri Lanka.

Profile Lines to Measure Flood Depths	250 m		500 m		750 m	
	25-year	50-year	25-year	50-year	25-year	50-year
Parliament Bridge	0.00	0.00	1.05	1.35	1.48	1.99
Ethul Kotte Bridge	1.85	2.66	1.17	1.79	1.38	2.16
Kimbulawala Bridge	0.00	0.00	0.00	0.00	0.00	0.00
Profile Line (PL) 4	0.00	0.00	1.61	2.01	0.00	0.00

extents and depths calculated as mentioned under the methodology, utilising Eq. (2) and Eq. (3). Table 4 presents EAD for RP floods of 5-year, 10-year, 25-year, and 50-year for the "before FMM" scenario.

The considered FMMs were implemented by SLLDC to reduce the flood damages within the Colombo Metropolitan Area, recognizing the area's commercial significance and economic importance. Under each RP, both the tangible loss and intangible loss were accounted for. From the calculations, it was evident that with the intensification of the flood inundation depth with the increase of the RP, there was a significant increase in the damage costs. Damage estimations for the "with FMM" condition were presented in Table 4, and by comparing the values in the adjacent columns, it was depicted that after the implementation of the measures, there was a drastic reduction in the estimated damage values that were calculated. Similarly, when damage estimations for favourable and unfavourable conditions were compared, an increase in damage values was shown during the unfavourable occasions, as the flow of flood water was further restricted. The percentage differences from damage reduction lie in the range of 39 % to 63 % when "without FMM" and "with FMM" scenarios were compared, and at the same time, low damages will result in enabling fast recovery. This approach helps to identify the absolute benefit of FMM and understand the actual estimated damage due to a flood under changing RPs. Further, as an extension of the study, reduced benefits can be compared with the construction costs of measures in the form of a benefit-to-cost ratio, and a clear representation of the benefit received by the implementation of FMMs can be taken. This approach will act as an indicator to make decisions regarding the selection of the most effective and economic measures that will reduce unnecessary costs covered by the authorities.

3.4. Investment viability analysis

Within the investment viability analysis, nine (9) implemented FMMs were taken into consideration (Table 5). Each FMM was analysed separately to identify the reduction of flood damage after the construction of the measure as mentioned in Section 2.3.4, and it was considered as the benefit acquired. Based on benefits and spent costs,

Table 4
Estimated flood damages (EAD in $Millions) for floods of different return periods for flood mitigation measures implemented in Colombo, Sri Lanka by SLLDC.

Loss classes	Favourable conditions		Unfavourable conditions	
	Without measures ($M)	With measures ($M)	Without measures ($M)	With measures ($M)
5-year Return Period				
Intangible loss (not accounted)	0.21	0.08	0.49	0.22
Intangible loss (accounted for)	0.69	0.34	0.90	0.46
10-year Return Period				
Intangible loss (not accounted)	0.83	0.38	2.38	1.45
Intangible loss (accounted for)	1.13	0.56	3.16	1.86
25-year Return Period				
Intangible loss (not accounted)	2.08	0.78	2.83	1.57
Intangible loss (accounted for)	3.69	0.97	5.04	2.26
50-year Return Period				
Intangible loss (not accounted)	2.51	1.58	3.42	1.89
Intangible loss (accounted for)	4.99	2.34	5.03	2.54

Table 5
Calculated NPV values and B/C ratios for implemented flood mitigation measures in Colombo, Sri Lanka by the Urban Water Management Center of SLLDC.

Implemented flood mitigation projects by SLLDC	Cost (Millions LKR)	Project commencement date	Annual maintenance cost (Millions LKR)	NPV	B/C ratio
Kolonnawa Canal Diversion	3,000	2021	11.12	2,499	2.60
St. Sebastian South Canal	1,225	2003	0.83	154	1.69
New Mutwal Tunnel	5,400	2021	20.02	4,492	1.95
Madiwela East Diversion	2,675	2021	2.50	562	1.73
Madiwela South Diversion	5,200	2021	18.35	4,123	2.96
North Lock Gates and Pumping Stations	5,100	2021	8.34	4,475	2.91
Greater Colombo Basin Storm Water Drainage Project	4,389	2003	5.67	641	2.23
Bolgoda Basin Storm Water Drainage Project	5,102	2003	1.53	720	2.22
Weras Ganga Storm Water Drainage Project	4,389	2003	2.22	641	2.09

NPV values and B/C ratios were calculated as in Table 5. The calculated NPV values and B/C ratios show that the implemented flood mitigation projects were economically profitable, with positive B/C ratios ranging from 1.69 to 2.96 and positive NPVs. Madiwela South Diversion and North Lock gates with pumping stations show the highest B/C ratios of 2.96 and 2.91, while St. Sebastian canal development, Madiwela East diversion and New Mutwal tunnel show moderate B/C cost ratios. Thus, based on the analysis, the considered FMMs can be justified as financially viable options for flood mitigation.

The methodology can also be applied to proposed FMMs to select the most viable investment that will bring more profits. Within the study, as the damage reductions were directly linked to the project benefit, the flood depth reduction and flood extent reductions through implementing proposed FMMs can be directly taken into account, creating a direct link between the effect of the FMM and investment viability. Thus, decision makers can use the approach as a sound option in selecting the most effective FMM.

3.5. Comparison with global studies

Comparable flood damage assessment studies have been conducted globally, yet key methodological gaps remain when contrasted with the present study. In Jakarta, [43] developed the Damagescanner-Jakarta model to estimate expected annual flood damages based on hazard, exposure, and vulnerability components using a grid-based approach. Similarly, in the Bago Region of Myanmar, [44] developed flood damage functions specific to house types using household surveys and simulated flood extents using the RRI (Rainfall–Runoff–Inundation) model. The focus of the study was on improving damage accuracy by considering building characteristics and evaluating damage reductions from adaptation options to residential buildings. In the Erasinos Basin, Greece, [45] developed a GIS-based tool to estimate direct flood damage to built-up and agricultural areas using relative depth–damage functions, with flood inundation mapping performed via HEC-RAS. While their approach shares methodological similarities with the present study, it focused solely on tangible damage estimation. However, none of these studies assessed the effectiveness or economic viability of flood mitigation measures, which constitutes a core contribution of the present research conducted in Colombo.

Focusing on the limitations of the current study, several simplifications and assumptions should be acknowledged. The land use was treated as static, without accounting for future urban expansion, and the effect of climate change was also not a focus within the study. Additionally, socio-economic exposure and vulnerability parameters were generalized by incorporating a fixed multiplier as a simplification attempt in the study. Despite these constraints, the integrated modeling framework remains robust for relative comparison of flood mitigation alternatives. Future research should address these limitations by incorporating dynamic land use projections, high-resolution socio-economic vulnerability data, and CMIP6-based climate scenarios to simulate evolving rainfall extremes. This would enhance the applicability and resilience of the framework under changing urban and climatic conditions.

4. Conclusions

The study provides a comprehensive evaluation of the application of multi-criteria flood hazard mapping, flood inundation mapping, and economic flood damage estimations to establish a strong basis for flood risk management in urban areas, Colombo, Sri Lanka, and Auckland, New Zealand. Considering Colombo, Sri Lanka's condition, under 100 mm/day rainfall, 47.55 % of the area is under moderate hazard conditions, and 11.36 % of the area is under high-hazard zones, where over 50 % of the study area is prone to urban floods. Focusing on Auckland, New Zealand, 22 % of the land extent shows an extreme hazard level, including the Auckland city limits, increasing the built environment

vulnerability. Both the executed case study areas display congested economic features with built-up area percentages of 85.6 % and 96 % for Colombo city limits, Sri Lanka and Auckland city limits, New Zealand, highlighting the need for proper FMMs to safeguard these built environments. Thus, similar hazard assessments can be conducted in urban cities that face the consequences of flooding to identify and classify hazard levels. As the next section of the study, flood inundation mapping for "with FMM" and "without FMM" was executed for selected Madiwela South Diversion, and a flood inundation depth reduction in the range of 9.2 % to 11.9 % was experienced at 50-year RP floods, suggesting the effect of FMM in depth reduction. The reduction of inundation depths directly affects the reduction of flood damage. Damage estimations under different flood inundation depths showed a percentage damage reduction of 39 % to 63 % with the reduction of inundation depths. Both the reductions in flood depths and damages demonstrate that strategic FMMs can simultaneously reduce physical flood impact and associated economic losses in densely built environments. Further financial indicators like NPV and B/C ratios can be used to analyse the financial viability of FMMs. From the calculations, it can be shown that all considered FMMs in Colombo are financially justifiable, with positive NPV values and B/C ratios ranging from 1.69 to 2.96. The integration of four (4) studies provides a robust data-driven framework for flood management.The integration of RP-based HEC-HMS and HEC-RAS models with flood damage estimation provides a reliable method to quantify economic losses in monetary terms. This approach enables a direct financial justification of flood mitigation measures, making it a practical and effective tool.

5. Recommendations

The study underscores the value of coupling of HEC-HMS and HEC-RAS models with vulnerability-based damage estimation and investment viability analysis, which is an approach that remains underutilized in many urban flood studies. This coupling enables the quantification of both physical and economic performance of flood mitigation measures, supporting evidence-based planning. This approach can be applied globally in identifying economic damages due to flooding, and it will support safeguarding communities against the growing urban flood risks, also facing the adversities due to climate change. Further, by prioritizing coordinated land-use planning, zoning regulations, and the integration of green infrastructure, cities can proactively reduce flood vulnerability and strengthen long-term urban resilience. These planning decisions should be informed by spatial assessments of flood extent and depth, as well as the economic feasibility of proposed mitigation measures, enabling evidence-based policy and investment. Additionally, machine learning (ML) techniques can be integrated with HEC-RAS simulation outputs to enable real-time, spatially explicit flood damage estimation platforms. These systems will have the ability to rapidly assess economic losses using flood depth maps, exposure layers, and vulnerability curves, offering critical support for operational risk management and emergency planning. Similar to the approach adopted by [46], for earthquake-induced slope instability, using Python-integrated safety factor analysis.

Relevance to resilience

The study makes a significant contribution to increasing urban resilience by addressing prevailing vulnerabilities within urban environments due to flooding. The methodology of the study was systematically formulated to generate data-driven, results-oriented decisions using the application of GIS-based hazard mapping, hydraulic modelling for inundation mapping and vulnerability curves in economic assessments. The hazard assessment was formulated to discover different hazard levels within the study areas of Colombo, Sri Lanka and Auckland, New Zealand, while the study can be applied to urban environments elsewhere facing similar urban floods. Simultaneous studies of flood inundation mapping and economic assessments provide a methodology flow chain to evaluate the effectiveness of structural flood mitigation measures in terms of flood inundation depth reduction and flood damage reduction. Under flood damage estimations, both tangible and intangible asset damages were comprehensively assessed to provide a holistic view of flood impacts. Even though the preliminary assessments were carried out for the selected pilot areas, they are scalable and adaptable for worldwide scenarios and directly support urban resilience improvements, enabling proactive planning and optimisation of flood mitigation measures, identifying unique characteristics in different research areas. This will reduce economic and societal costs due to flooding and enable a rapid recovery, establishing city resilience.

CRediT authorship contribution statement

Paboda Jayawardane: Writing – review & editing, Writing – original draft, Visualization, Validation, Software, Methodology, Formal analysis. **Lalith Rajapakse:** Writing – review & editing, Supervision, Resources, Project administration, Conceptualization. **Chandana Siriwardana:** Writing – review & editing, Supervision, Project administration, Conceptualization.

Conflict of interest statement

The authors declare no conflicts of interest related to this study.

Acknowledgement

The Sri Lanka Land Development Corporation (SLLDC) is gratefully acknowledged for its valuable support in providing data and insights related to structural flood mitigation measures, which were instrumental in conducting the study.

References

[1] Agonafir C, Lakhankar T, Khanbilvardi R, Krakauer N, Radell D, Devineni N. A review of recent advances in urban flood research. Water Secur 2023;19:100141. https://doi.org/10.1016/j.wasec.2023.100141.
[2] Li D, et al. Urban rainfall-runoff flooding response for development activities in new urbanized areas based on a novel distributed coupled model. Urban Clim 2023;51:101628. https://doi.org/10.1016/j.uclim.2023.101628.
[3] Zhao B, Tang Y, Wang C, Zhang S, Soga K. Evaluating the flooding level impacts on urban metro networks and travel demand: behavioral analyses, agent-based simulation, and large-scale case study. Resilient Cities Struct 2022;1(3):12–23. https://doi.org/10.1016/j.rcns.2022.10.004.
[4] Youssef AM, Pradhan B, Gaber AFD, Buchroithner MF. Geomorphological hazard analysis along the Egyptian Red Sea coast between Safaga and Quseir. Nat Hazards Earth Syst Sci 2009;9(3):751–66. https://doi.org/10.5194/nhess-9-751-2009.
[5] Cook S, Van Roon M, Ehrenfried L, LaGro J, Yu Q. WSUD 'best in class'—case studies from Australia, New Zealand, United States, Europe, and Asia. Approaches to water sensitive urban design. Elsevier; 2019. p. 561–85. https://doi.org/10.1016/B978-0-12-812843-5.00027-7.
[6] Khan MYA, ElKashouty M, Subyani AM, Tian F. Flash flood assessment and management for sustainable development using geospatial technology and WMS models in Abha City, Aseer Region, Saudi Arabia. Sustainability 2022;14(16):10430. https://doi.org/10.3390/su141610430.
[7] Cooper R. Hurricane Helene recovery: revised damage and needs assessment. Office of state budget and management. North Carolina; 2024.
[8] Gupta K. Challenges in developing urban flood resilience in India. Phil Trans R Soc A 2020;378(2168). https://doi.org/10.1098/rsta.2019.0211. 20190211.
[9] Bansal N, Mukherjee M, Gairola A. Evaluating urban flood hazard index (UFHI) of Dehradun city using GIS and multi-criteria decision analysis. Model Earth Syst Environ 2022;8(3):4051–64. https://doi.org/10.1007/s40808-021-01348-5.
[10] Randil C, Siriwardana C, Sandaruwan Rathnayaka B. A statistical method for pre-estimating impacts from a disaster: a case study of floods in Kaduwela, Sri Lanka. Int J Disaster Risk Reduct 2022;76:103010. https://doi.org/10.1016/j.ijdrr.2022.103010.
[11] Aldridge J, Bell RG. Climate change impacts to extreme weather events associated with insured losses in New Zealand: a review. Env Res: Clim 2024. https://doi.org/10.1088/2752-5295/ada1f0.
[12] T. I. Eldho, "Chapter 12 - urban flood management in coastal regions using numerical simulation and geographic information system," *Integr Disaster Sci Manag.*, vol. Part II, pp. 205–219, doi: http://doi.org/10.1016/B978-0-12-812056-9.00012-9.

[13] Glago FJ. Flood disaster hazards; causes, impacts and management: a state-of-the-art review. In: Noroozinejad Farsangi E, editor. Natural hazards - impacts, adjustments and resilience. IntechOpen; 2021. https://doi.org/10.5772/intechopen.95048.
[14] Schweckendiek T, editor. Comprehensive flood risk management: research for policy and practice. CRC Press; 2012. https://doi.org/10.1201/b13715.
[15] Kilsedar CE, Fissore F, Pirotti F, Brovelli MA. Extraction and visualization of 3d building models in urban areas for flood simulation. Int Arch Photogramm Remote Sens Spat Inf Sci 2019;XLII-2/W11:669–73. https://doi.org/10.5194/isprs-archives-XLII-2-W11-669-2019.
[16] Prashar N, Lakra HS, Shaw R, Kaur H. Urban flood resilience: a comprehensive review of assessment methods, tools, and techniques to manage disaster. Prog Disaster Sci 2023;20:100299. https://doi.org/10.1016/j.pdisas.2023.100299.
[17] Huang H, Zhang D, Huang Z. Resilience of city underground infrastructure under multi-hazards impact: from structural level to network level. Resilient Cities Struct 2022;1(2):76–86. https://doi.org/10.1016/j.rcns.2022.07.003.
[18] Dui H, Cao T, Wang F. Digital twin-based resilience evaluation and intelligent strategies of smart urban water distribution networks for emergency management. Resilient Cities Struct 2025;4(1):41–52. https://doi.org/10.1016/j.rcns.2025.02.001.
[19] Huang J, Wen H, Li Z, Zhang Y. Landslide-oriented disaster resilience evaluation in mountainous cities: a case study in Chongqing, China. Resilient Cities Struct 2024;3(4):34–51. https://doi.org/10.1016/j.rcns.2024.10.001.
[20] Rathnayaka B, Siriwardana C, Robert D, Amaratunga D, Setunge S. Improving the resilience of critical infrastructures: evidence-based insights from a systematic literature review. Int J Disaster Risk Reduct 2022;78:103123. https://doi.org/10.1016/j.ijdrr.2022.103123.
[21] Agonafir C, Lakhankar T, Khanbilvardi R, Krakauer N, Radell D, Devineni N. A review of recent advances in urban flood research. Water Secur 2023;19:100141. https://doi.org/10.1016/j.wasec.2023.100141.
[22] He J, Zhang L, Xiao T, Chen C. Emergency risk management for landslide dam breaks in 2018 on the Yangtze River, China. Resilient Cities Struct 2022;1(3):1–11. https://doi.org/10.1016/j.rcns.2022.10.003.
[23] Hdeib R, Aouad M. Rainwater harvesting systems: an urban flood risk mitigation measure in arid areas. Water Sci Eng 2023;16(3):219–25. https://doi.org/10.1016/j.wse.2023.04.004.
[24] Pinelli J-P, Pita G, Gurley K, Torkian B, Hamid S, Subramanian C. Damage characterization: application to florida public hurricane loss model. Nat Hazards Rev 2011;12(4):190–5. https://doi.org/10.1061/(ASCE)NH.1527-6996.0000051.
[25] Paleo-Torres A, et al. Vulnerability of Florida residential structures to hurricane-induced coastal flood. Eng Struct 2020;220:111004. https://doi.org/10.1016/j.engstruct.2020.111004.
[26] Baradaranshoraka M, Pinelli J-P, Gurley K, Peng X, Zhao M. Hurricane wind versus storm surge damage in the context of a risk prediction model. J Struct Eng 2017;143(9):04017103. https://doi.org/10.1061/(ASCE)ST.1943-541X.0001824.
[27] Hinge G, Hamouda MA, Mohamed MM. Flash flood susceptibility modelling using soft computing-based approaches: from bibliometric to meta-data analysis and future research directions. Water 2024;16(1):173. https://doi.org/10.3390/w16010173.
[28] Buta C, Mihai G, Stănescu M. Flood risk assessment based on flood hazard and vulnerability indexes. Ovidius Univ Ann Constanta - Ser Civ Eng 2020;22(1):127–37. https://doi.org/10.2478/ouacsce-2020-0014.
[29] Ahmed I, Das (Pan) N, Debnath J, Bhowmik M, Bhattacharjee S. Flood hazard zonation using GIS-based multi-parametric analytical hierarchy process. Geosyst Geoenviron 2024;3(2):100250. https://doi.org/10.1016/j.geogeo.2023.100250.
[30] A. D. S. Gunawardana and C. Eng, "Development of rainfall intensity-duration-frequency (IDF) curves for Colombo, Sri Lanka".
[31] Scharffenberg WA, Fleming MJ. Hydrologic modeling system HEC-HMS: user's manual. US Army Corps of Engineers, Hydrologic Engineering Center; 2006.
[32] Sampath DS, Weerakoon SB, Herath S. HEC-HMS model for runoff simulation in a tropical catchment with intra-basin diversions – case study of the Deduru Oya river basin, Sri Lanka. Engineer 2015;48(1):1. https://doi.org/10.4038/engineer.v48i1.6843.
[33] HEC-RAS Manual (2016) HEC-RAS, hydraulic, reference manual, hydrologic engineering centre, Davis Version 5.0.
[34] Nkeki FN, Bello EI, Agbaje IG. Flood risk mapping and urban infrastructural susceptibility assessment using a GIS and analytic hierarchical raster fusion approach in the Ona River Basin, Nigeria. Int J Disaster Risk Reduct 2022;77:103097. https://doi.org/10.1016/j.ijdrr.2022.103097.
[35] AL-Hussein AAM, Khan S, Ncibi K, Hamdi N, Hamed Y. Flood analysis using HEC-RAS and HEC-HMS: a case study of khazir river (Middle East—Northern Iraq). Water 2022;14(22):3779. https://doi.org/10.3390/w14223779.
[36] Weerasinghe KM, Gehrels H, Arambepola NMSI, Vajja HP, Herath JMK, Atapattu KB. Qualitative flood risk assessment for the western province of Sri Lanka. Procedia Eng 2018;212:503–10. https://doi.org/10.1016/j.proeng.2018.01.065.
[37] Moufar M, Perera E. Floods and countermeasures impact assessment for the metro Colombo Canal system, Sri Lanka. Hydrology 2018;5(1):11. https://doi.org/10.3390/hydrology5010011.
[38] Dias P, et al. Development of damage functions for flood risk assessment in the city of Colombo (Sri Lanka). Procedia Eng 2018;212:332–9. https://doi.org/10.1016/j.proeng.2018.01.043.
[39] Wagenaar DJ, et al. Evaluating adaptation measures for reducing flood risk: a case study in the city of Colombo, Sri Lanka. Int J Disaster Risk Reduct 2019;37:101162. https://doi.org/10.1016/j.ijdrr.2019.101162.
[40] Vilier JJTA. Assessment of the costs of business interruption caused by large-scale floods: a comparison of methods. Delft University of Technology; 2013.
[41] Molinari D, et al. Cost–benefit analysis of flood mitigation measures: a case study employing high-performance hydraulic and damage modelling. Nat Hazards 2021;108(3):3061–84. https://doi.org/10.1007/s11069-021-04814-6.
[42] Haer T, et al. Economic evaluation of climate risk adaptation strategies: cost-benefit analysis of flood protection in Tabasco, Mexico. Atm 2017;30(2):101–20. https://doi.org/10.20937/ATM.2017.30.02.03.
[43] Budiyono Y, Aerts JCJH, Tollenaar D, Ward P. River flood risk in Jakarta under scenarios of future change. Nat Hazards Earth Syst Sci 2015;(16):757–74. https://doi.org/10.5194/nhessd-3-4435-2015.
[44] Shrestha BB, Kawasaki A, Zin WW. Development of flood damage assessment method for residential areas considering various house types for Bago Region of Myanmar. Int J Disaster Risk Reduct 2021;66:102602. https://doi.org/10.1016/j.ijdrr.2021.102602.
[45] Pistrika A. Flood damage estimation based on flood simulation scenarios and a GIS platform. Eur Water 2010;(30):3–11.
[46] W. Yiheng, M.M. Kassem, and F.M. Nazri, "Evaluating earthquake-induced slope instability via safety factor analysis: advance sarma method with python integration," in *Selected articles from the 8th international conference on architecture and civil engineering*, vol. 635, E.M. Nia, M. Awang, M.F.N. Aulady, M. Traykova, and L. Yola, in Lecture Notes in Civil Engineering, vol. 635., Singapore: Springer Nature Singapore, 2025, pp. 20–29. doi: 10.1007/978-981-96-5654-7_3.